Proceedings of CONF-MCEE 2026 Symposium: Advances in Sustainable Aviation and Aerospace Vehicle Automation
DOI: 10.54254/2755-2721/2026.KA30031

Feasibility of Using Flexible Pressure Sensors for Medical Monitoring

Sirui Li

School of Engineering, University of Edinburgh, Edinburgh, United Kingdom
18620147831@163.com

Abstract. Growing demand for unobtrusive, continuous physiological monitoring in healthcare, rehabilitation and home settings highlights the need for thin, comfortable, and accurate pressure sensing. This paper investigates a flexible, multilayer Inductor-capacitor pressure sensor and a portable readout scheme for medical detection. The study aims to verify whether resonant-frequency shifts of the sensor can be robustly converted to pressure values outside laboratory conditions. This study derives a closed-form mapping from a parallel-plate and axial-compression model, then implements a portable frequency-sweep readout (frequency response analyzer with directional coupler) to track resonance. Bench measurements on prototype sensors use baseline/load tests, narrowband sweeps, and Lorentzian fitting to estimate Q, f_r and uncertainty; results are compared with conventional instrumentation to assess agreement. The findings show identifiable amplitude dips and phase transitions near resonance, allowing frequency estimation with low dispersion and thus reliable pressure reconstruction after calibration. The portable pathway reduces cost and deployment complexity while maintaining practical accuracy, supporting applications such as abdominal respiration tracking and compression-therapy feedback. Overall, the work demonstrates the feasibility of flexible LC sensors coupled with a portable readout for clinical and home pressure monitoring.

Keywords: Resonant frequency, Compression therapy, Sensor, Inductor-capacitor circuit

1. Introduction

With people's increasing concern for health and the growing demand for precise physiological monitoring in the fields of medical care, rehabilitation, and fitness, various types of physical examinations have received widespread attention as an important means of detecting physiological indicators [1]. However, most existing detection methods rely on large and complex detection equipment in hospitals, or lack accuracy and portability, making it difficult to meet the needs of daily use and diverse scenarios [2]. Therefore, the development of a high-precision, portable and easy-to-use medical sensor is of great practical significance and will provide strong support for personal health management, clinical auxiliary diagnosis, sports training guidance, etc [3]. This article mainly focuses on sensors used to detect pressure-related parameters such as abdominal breathing and venous thrombosis. Beyond practical deployment, this work has broader significance for healthcare and related industries. By demonstrating a thin, comfortable, and low-cost pressure-

© 2026 The Authors. This is an open access article distributed under the terms of the Creative Commons Attribution License 4.0 (https://creativecommons.org/licenses/by/4.0/).

DOI: 10.54254/2755-2721/2026.KA30031

sensing route with portable readout, it lowers the barrier to continuous monitoring in clinical wards, home care, and rehabilitation, enabling earlier risk detection (e.g., DVT) and more precise, feedback-guided compression therapy [4].

2. Flexible pressure sensor

Flexible pressure sensors typically use a "sandwich" multilayer structure: upper and lower metal spiral coils and a microstructure elastic medium in the middle form an adjustable LC resonance unit [5]. The device is typically only about 150um thick and can be bent 180 degrees. It is often used in conjunction with smart clothing to assist in detection [6]. Figure 1 shows the schematic of the proposed capacitive pressure sensor; the top (i) and bottom (iii) layers are the Ti/Cu-coated glass layers used as parallel capacitor plates and to encapsulate the microstructure elastomeric blend layer (ii). The geometry of the latter layer is defined by the spacing a (30 and 50 m) and dimension b (35 and 100 m, respectively) of the square micro-pillar array features.

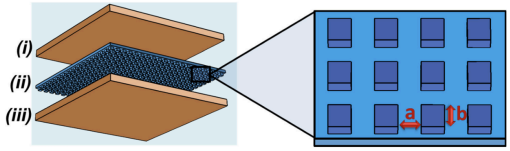


Figure 1. Schematic of the proposed capacitive pressure sensor

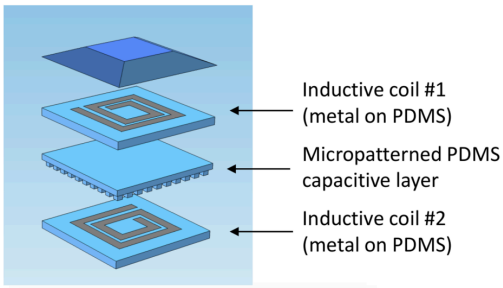


Figure 2. Layers of LC pressure sensor

Figure 2 shows the device's three-layer "sandwich" structure from another angle: a planar spiral inductor coil is fabricated on top and bottom PDMS films; the middle PDMS elastic dielectric layer, with micro-bumps/micro-pillars on its surface, serves as a compressible capacitor. Once assembled, the upper and lower metal layers provide both inductance L and, together with the dielectric in the middle, capacitance C, forming an LC resonant unit.

DOI: 10.54254/2755-2721/2026.KA30031

2.1. Introduction to RLC resonant circuit

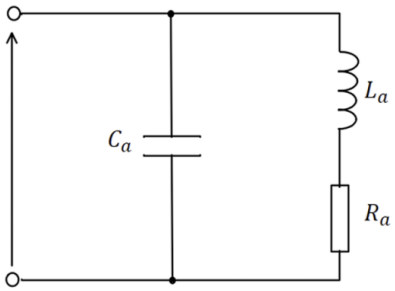


Figure 3. Equivalent circuit of LC circuit

Flexible pressure sensors are electrically equivalent to a first-order lossy resonant circuit, which is shown in Figure 3: the inductance, L, is provided by a planar spiral coil; the capacitance, C, consists of two conductor layers with a dielectric layer between them; and the loss resistor, R, combines metal resistance, dielectric loss, and radiation loss. When compressed, changes in dielectric thickness and equivalent permittivity cause C to shift, resulting in a shift in the resonant frequency [7-8].

Resonant Frequency:

$$fs = \frac{1}{2\pi\sqrt{\mathrm{LC}}} \tag{1}$$

Parallel plate capacitor:

$$C = \varepsilon_r\varepsilon_0\frac{\mathrm{A}}{\mathrm{d}} \tag{2}$$

Where A is the effective overlapping area of the plates, d is the distance between the two plates, and εr is the relative dielectric constant of the medium.

2.2. Introduction to the detection system

To effectively establish a quantitative relationship between pressure and frequency, the following reasonable assumptions are necessary [9]:

A. The flexible pressure sensor is electrically equivalent to a first-order lossy resonant circuit (RLC). The planar spiral coil provides inductance L, while the upper and lower electrodes and the compressible dielectric layer in the middle form capacitance C The loss resistance R affects the quality factor, but the first-order shift in the resonant center frequency is negligible.

B. The dielectric layer is axially compressed, acting as a "linear spring" or spring array. Under small deformation conditions, its thickness compression is approximately linear with the external force.

C. The effective electrode overlap area is A and the dielectric equivalent dielectric constant is $\varepsilon = \varepsilon_r\varepsilon_0$

The symbols and meanings used in this paper are as follows:

P : Uniform pressure acting on area A ;

$\mathrm{d(P)}$: Compressed dielectric layer thickness;

$\mathrm{C(P)}$: Compressed sensor capacitance;

DOI: 10.54254/2755-2721/2026.KA30031

$f(P)$: Resonant frequency at pressure P ;

k_{eff} : Equivalent axial stiffness of the dielectric layer;

Q : Quality factor (used only to characterize the sharpness of the curve and not involved in the calculation of the center frequency).

The uniform pressure P on the action area A , the total external force $F = PA$. The equivalent stiffness k_{eff} is used to characterize the axial resistance of the dielectric layer, and the thickness compression is

$$\Delta d = \frac{F}{k_{eff}} = \frac{PA}{k_{eff}} \tag{3}$$

$$d(P) = d_0 - \Delta d = d_0 - \frac{PA}{k_{eff}} \tag{4}$$

Under the parallel plate dominant approximation (edge effects are incorporated into the constant correction), the capacitance:

$$C(P) = \frac{\varepsilon A}{d(P)} = \frac{A}{d_0 - \frac{PA}{k_{eff}}} \tag{5}$$

Bringing it back to the formula for resonant frequency, we can find that:

$$f(P) = \frac{1}{2\pi}\sqrt{\frac{d_0 - \frac{PA}{k_{eff}}}{L\varepsilon A}} \tag{6}$$

By reversing the above equation, we can get the closed-form relationship between voltage and frequency:

$$P(f) = \frac{k_{eff}}{A} d_0 - k_{eff}\left(2\pi\right)^2 L\varepsilon f^2 \tag{7}$$

The engineering significance of this expression is clear: once the parameters $\{L, \varepsilon, d_0, k_{eff}\}$ or their combination constants are determined, the corresponding pressure P can be directly calculated from the measured frequency f.

3. Expandable functional modules

3.1. Wireless detection

Passive wireless sensors—such as resonance-type devices—are widely used for pressure, temperature, and strain monitoring. Lacking an internal power source, they draw energy from the electromagnetic field emitted by a nearby reader antenna in the near or far field. In passive sensing, the sensor coil or antenna and a reader antenna are electromagnetically coupled (via mutual inductance M or capacitive coupling). This coupling can be modeled similarly to a transformer, where:

$$M = k\sqrt{L_a L_s} \tag{8}$$

DOI: 10.54254/2755-2721/2026.KA30031

With La being the reader- antenna inductance and k the coupling coefficient ($0\leq \mathrm{k} \leq 1$).

The flexible sensor itself is equivalent to a first-order lossy resonant circuit (RLC), whose resonant frequency drifts with the capacitance change caused by pressure. To achieve contactless readout, a readout coil/antenna is placed near the sensor to form near-field mutual inductance coupling with the sensor. The equivalent voltage equation for the two circuits (readout end "1" and sensor end "2") is:

$$\left\{\begin{array}{c} \mathrm{V}_1=(\mathrm{Ra}+\mathrm{j}\omega\mathrm{La})Ia+\ j\omega MIs \\ 0=(\mathrm{Rs}+\mathrm{j}\omega\mathrm{Ls})Is-\ \frac{1}{\mathrm{j}\omega\mathrm{Cs}}Is+j\omega MIa \end{array}\right\} \tag{9}$$

As can be seen from the second relationship, the sensor circuit behaves as a passive load, its energy acquisition relying solely on the mutual inductance and the coupling between the read/write terminals. The input impedance of the read port is defined as:

$$Zin\left(\omega\right)=\frac{\mathrm{V1}}{\mathrm{I_a}} \tag{10}$$

Eliminates Is from the system of equations, we obtain:

$$\mathrm{Z_{in}}\left(\omega\right)=Ra+j\omega La+\frac{\omega^2\mathrm{M}^2}{\mathrm{Rs}+\mathrm{j}\left(\omega\mathrm{Ls}-\frac{1}{\omega\mathrm{Cs}}\right)} \tag{11}$$

When ω approaches the natural frequency ω_s, the denominator of the second term decreases at series resonance and increases at parallel resonance, forming a clearly discernible feature on $\mathrm{Z_{in}}(\omega)$ [10].

3.1.1. Phase dip and real-part peak

A. Phase dip

When plotting the phase of $\angle\mathrm{Z_{in}}(\omega)$ as a function of frequency, a steep "dip" often appears near resonance, potentially exceeding 0°. The frequency corresponding to this characteristic can directly indicate the coupling resonance point of the sensor.

B. Real-part peak

Another approach is to track $\mathrm{R_e}\ \{\mathrm{Zin}(\omega)\}$. A local maximum (or minimum) around ωs can similarly reveal the resonant frequency.

As pressure changes the sensor parameters ($\mathrm{L_s}, \mathrm{C_s}$), these impedance-based features shift in frequency, enabling a remote measure of pressure via the amount of frequency offset Δf.

3.1.2. Single-port scattering parameter

Define:

$$S11\left(\omega\right)=\frac{\mathrm{Zin}(\omega)-\mathrm{Z0}}{\mathrm{Zin}(\omega)+\mathrm{Z0}} \tag{12}$$

Where $\mathrm{Z0}$ is characteristic impedance of the instrument and cables, and Zin is the input impedance derived above.

DOI: 10.54254/2755-2721/2026.KA30031

Amplitude is the magnitude | S11(f)|, usually shows a significant "valley" near the sensor resonance, which is due to the strong absorption of energy by the resonant circuit and the sudden change in mismatch conditions. Phase ∠S11(f) often undergoes rapid transitions near the same frequency; this phase shift can also be used to precisely locate the resonant position.

Based on the sensor parameters, select an appropriate sweep bandwidth and simultaneously measure the phase and amplitude of S11 using a vector network analyzer (VNA) or other scannable RF equipment. Plot the obtained discrete results as curves using other plotting methods. The frequency corresponding to the deepest amplitude "valley" or the frequency of the phase abrupt change can be denoted as f_{means}. When the coupling coefficient is appropriate, f_{means} is close to the intrinsic resonant frequency f_s during the period, and therefore can be used as the measurement result of the sensor's resonant frequency [11].

3.2. Portable readout system

3.2.1. Background information for readout system

Flexible passive pressure sensors are typically based on the RLC resonance mechanism: an external readout uses near field coupling to identify the sensor's resonant characteristics (amplitude dips/phase jumps) in the swept frequency response, thereby acquiring the resonant frequency and mapping it to pressure. Traditionally, this type of readout relies on a vector network analyser (VNA) to perform one- or two-port S-parameter measurements. VNAs offer wide bandwidth, high dynamic range, and rigorous calibration/de-embedding capabilities, making them the "gold standard" for research-grade characterization. However, in non-laboratory environments such as clinical bedside, rehabilitation training, home scenarios, or large-scale field testing, VNAs face significant limitations: large size, high price, complex usage and calibration processes, and sensitivity to power supply and cable/termination conditions, making it difficult to meet the needs of long-term, continuous, low-intrusion monitoring.

3.2.2. Motivation for portable readout devices

To enable “anytime, anywhere” pressure monitoring and closed-loop regulation, this work proposes migrating the readout chain from laboratory-grade instrumentation to portable platforms. Concretely, we target an all-in-one device that integrates a frequency-response analyser and function generator with on-board data acquisition and employs a directional coupler to realize reflective measurements. This architectural shift is driven by practical constraints in real-world deployments and the performance requirements of medical sensing.

First, application accessibility is paramount. In clinical wards, home rehabilitation, sports training, and field assessments, devices must be compact, easy to deploy, and low-maintenance, and must operate reliably under limited space and power conditions. A portable readout satisfies these constraints while preserving the essential capability to localize the sensor’s resonance.

Second, continuous and long-term monitoring is best supported by portable platforms that can be coupled to wearable sensors. Such coupling enables high-frequency and extended-duration measurement schedules, thereby capturing pressure fluctuations and inter-individual differences during daily activities—signals that are often missed by intermittent, clinic-only measurements.

Third, cost and scalability considerations favor portability. Relative to vector network analyses (VNAs), portable readouts substantially reduce procurement and maintenance costs and are easier to deploy at scale for batch data collection and management, a prerequisite for population-level studies.

DOI: 10.54254/2755-2721/2026.KA30031

Fourth, portable devices offer superior engineering integration. Programmable interfaces and embedded software ecosystems facilitate seamless linkage with host computers, mobile terminals, and hospital information systems, supporting real-time visualization, cloud storage, and remote evaluation.

Finally, the proposed approach aligns with application demand. Most medical and rehabilitation scenarios require robust localization of the resonant frequency and its mapping to pressure, rather than absolute, rigorously calibrated S-parameters over a wide band. By focusing on these core requirements, the portable platform markedly reduces system complexity while maintaining clinically useful accuracy.

3.2.3. Advantages and limitations

Advantages of Portable Readout Devices over Traditional VNAs:

(1) System and Deployment

Portable readout devices offer superior portability and scenario adaptability. Their small size and low mass make them suitable for bedside, outpatient, home, and field use, obviating the need for dedicated equipment rooms or rack-mount infrastructure. Operational procedures are streamlined, enabling rapid setup by engineers and clinical staff without RF specialization. In practice, usable metrics can be obtained through a succinct baseline → load → fit workflow.

(2) Performance and Usability

A task-focused design emphasizes the two core functions—resonant-frequency localization and pressure mapping—delivering clinically practical accuracy without imposing stringent requirements on absolute, wideband S-parameters. With directional couplers, moderate coupling, and narrowband, high-density sweeps, the system achieves clearly discernible amplitude dips and phase transitions along with low frequency-estimation variance. Built-in or host-side modules for curve fitting, sensitivity computation, and uncertainty quantification convert raw measurements directly into pressure values with confidence intervals, shortening the path from waveforms to actionable clinical or engineering indicators.

(3) Cost and Scalability

Acquisition and maintenance costs are markedly lower than for VNAs, enabling more measurement sites and broader user coverage. Portable platforms integrate readily with mobile and cloud ecosystems, supporting batch acquisition, remote quality control, and over-the-air software updates. Open control interfaces and SDKs facilitate secondary development, including robust frequency-tracking algorithms and adaptive sweep strategies, and simplify integration with third-party systems.

(4) Reliability and Operations

Even in non-ideal environments lacking strict shielding or anechoic conditions, a strategy of normalization/differencing, repeated measurements, and rigid fixture yields stable reads. Routine operation relies on relative calibration and baseline management rather than exhaustive OSL procedures, preserving confidence in results while reducing operational and maintenance burden.

Despite these benefits, portable readout links are typically quasi-reflectometry rather than fully calibrated S-parameter measurements. Cross-device or cross-batch comparisons therefore require relative calibration and de-embedding to a unified reference plane. Performance depends on geometric alignment and the coupling coefficient k; fixed fixtures and recorded pose/spacing are recommended. When sensor losses are high (low Q), resonance features weaken, increasing frequency-estimate uncertainty; mitigation includes microstructure/material optimization, higher coupling and spectral point density, and phase-based fitting. Finally, temperature and time-

DOI: 10.54254/2755-2721/2026.KA30031

dependent effects (e.g., viscoelastic creep) warrant temperature logging, a standardized load–hold–read window, and explicit compensation terms in calibration.

4. Conclusion

This paper presents a complete methodological framework for "flexible passive pressure sensor - closed-form mapping from frequency to pressure-portable readout link-uncertainty quantification". Compared with the VNA path, the portable readout meets the core requirements of frequency positioning and pressure estimation at a lower cost and complexity, making it suitable for long-term monitoring at bedside, at home, and in the field. Nevertheless, several avenues remain for improvement. First, this study does not deeply examine temperature drift, viscoelastic creep of the elastomer, or posture-dependent coupling—factors that can bias frequency estimates; future work should incorporate physics-based compensation and controlled stress–relaxation tests. Second, this research did not perform absolute one-port OSL calibration or full de-embedding to the coil reference plane; adding these would enable stricter cross-platform comparability. Third, the sensor microstructure/Q-factor optimization and long-term repeatability under bending/sweat were only preliminarily assessed; accelerated aging and human-in-the-loop trials are needed.

Subsequent work can be deepened in three aspects: (1) high-Q and high-sensitivity microstructure design to further reduce σf and σP; (2) adaptive frequency sweep and robust frequency estimation algorithm to improve stability in low signal-to-noise ratio and drift environments; (3) system-level compensation (temperature/viscoelastic/coupling attitude) and standardized calibration process to support consistency evaluation across batches and multi-centre applications.

References

[1] K. Munirathinam, et al. “Recent progress on flexible capacitive pressure sensors, ” Advanced Materials Technologies, 2021.
[2] B. Xu, et al. “Radio-frequency resonator-based flexible wireless sensors for biomedical applications, ” Micromachines, 2022.
[3] A. Sachdeva, et al. “Graduated compression stockings for prevention of deep vein thrombosis, ” Cochrane Database of Systematic Reviews, 2018/2021 update.
[4] C. Qian, et al. “Wireless and battery-free LC sensor for interstitial fluid pressure monitoring, ” Biosensors and Bioelectronics, 2024.
[5] W.-J. Deng, L.-F. Wang, L. Dong, Q.-A. Huang. “LC wireless sensitive pressure sensors with microstructured PDMS dielectric layers for wound monitoring, ” IEEE Sensors Journal, 2018.
[6] Z. Sun, et al. “Flexible wireless passive LC pressure sensor: design methodology and cost-effective preparation, ” Micromachines, 2021.
[7] H. Kou, et al. “Wireless wide-range pressure sensor based on graphene/PDMS sponge, ” Scientific Reports, 2019.
[8] S. Charkhabi, et al. “Monitoring wound health through bandages with passive LC sensors, ” ACS Sensors, 2020.
[9] S. Li, et al. “Iontronic-capacitance-enhanced LC wireless passive pressure sensor, ” Applied Physics Letters, 2023.
[10] F. Caspers. “RF engineering basic concepts: S-parameters, ” CERN Note, 2012.
[11] S. Amakawa, et al. “Demystifying complex-referenced S-parameters, ” IEICE Transactions on Electronics, 2016.